FEB 3 1986

I28.23: 8997

RI 8997

631-A COMPLETED 19

Bureau of Mines Report of Investigations/1985

ORIGINAL

# Utilization of Simulated Coal Gases for Reducing Iron Oxide Pellets

By Larry A. Haas, John C. Nigro, and Robert K. Zahl

UNITED STATES DEPARTMENT OF THE INTERIOR

BUREAU OF MINES 75TH ANNIVERSARY

BEST COPY AVAILABLE

Report of Investigations 8997

# Utilization of Simulated Coal Gases for Reducing Iron Oxide Pellets

By Larry A. Haas, John C. Nigro, and Robert K. Zahl

UNITED STATES DEPARTMENT OF THE INTERIOR
Donald Paul Hodel, Secretary

BUREAU OF MINES
Robert C. Horton, Director

I

BEST COPY AVAILABLE

Library of Congress Cataloging in Publication Data:

Haas, L. A. (Larry A.)

Utilization of simulated coal gases for reducing iron oxide pellets.

(Report of investigations / United States Department of the Interior, Bureau of Mines ; 8997)

Bibliography: p. 14.

Supt. of Docs. no.: I 28.23: 8997.

1. Iron–Metallurgy. 2. Iron oxides. 3. Reduction, Chemical. 4. Gas. I. Nigro, John C. II. Zahl, Robert K. III. Title. IV. Series: Report of investigations (United States. Bureau of Mines) ; 8997.

TN23.U43 [TN707] 622s [669'.14] 85-600202

BEST COPY AVAILABLE

CONTENTS


| | Page |
|---|---|
| Abstract | 1 |
| Introduction | 2 |
| Acknowledgments | 3 |
| Experimental work | 3 |
| Materials | 3 |
| Procedure | 3 |
| Results and discussion | 4 |
| Single-reductant gas mixtures | 4 |
| Simulated reformed and coal-gas mixtures | 9 |
| Evaluation of reduced pellets | 12 |
| Conclusions | 13 |
| References | 14 |


ILLUSTRATIONS


| | | |
|---|---|---|
| 1. | Experimental equipment used in reduction studies of iron oxide pellets | 3 |
| 2. | Influence of gas flow rates on percent reduction with 100 pct $H_2$ at 900° C | 4 |
| 3. | Comparison of reduction-rate data using various normalized reduction functions | 5 |
| 4. | Arrhenius plots with 100 pct $H_2$, CO, or $CH_4$ | 5 |
| 5. | Plot of logarithm of reductant pressure and reduction rate at 900° C | 6 |
| 6. | Influence of $CO_2$ and CO on reduction at 900° C | 7 |
| 7. | Equilibrium diagram of iron in presence of various gases | 7 |
| 8. | Influence of water vapor and $CO_2$ on reduction rate constant at 900° C | 8 |
| 9. | Influence of water vapor in $H_2$ on reduction at 900° C | 8 |
| 10. | Dependence of calculated and experimental reduction rate constants on gas composition and temperature | 11 |
| 11. | Dependence of the 90-pct reduction time on type of reducing gas and temperature | 12 |
| 12. | Pellet pore size distribution before and after reduction | 13 |


TABLES


| | | |
|---|---|---|
| 1. | Partial analyses of actual and simulated reducing-gas mixtures | 2 |
| 2. | Partial chemical analyses of fired iron oxide pellets before reduction | 3 |
| 3. | Chemical and physical properties of reduced iron oxide pellets | 10 |




BEST COPY AVAILABLE

UNIT OF MEASURE ABBREVIATIONS USED IN THIS REPORT

| | | | |
|---|---|---|---|
| atm | atmosphere | kcal/mol | kilocalorie per mole |
| Btu | British thermal unit | kg | kilogram |
| °C | degree Celsius | lb | pound |
| cm | centimeter | μm | micrometer |
| g | gram | mm | millimeter |
| $g/cm^3$ | gram per cubic centimeter | min | minute |
| | | pct | percent |
| h | hour | scf | standard cubic foot |
| in | inch | SLM | standard liter per minute |
| K | kelvin | | |

BEST COPY AVAILABLE

# UTILIZATION OF SIMULATED COAL GASES FOR REDUCING IRON OXIDE PELLETS

By Larry A. Haas,[1] John C. Nigro,[2] and Robert K. Zahl[3]


## ABSTRACT

The Bureau of Mines is investigating the use of complex gas mixtures, such as would be produced by coal gasification, for reducing iron oxide pellets. A semiempirical model was developed to predict a priori the reduction rate of an iron oxide pellet in a laboratory tube furnace with simulated coal gases at a total pressure of 1 atm. The model uses partial pressures of $H_2$, CO, $CO_2$, $CH_4$ (methane), water vapor, and a temperature-dependent term to predict the rate of reaction. The reduction rate (weight loss per unit of time) was determined with a thermogravimetric apparatus (TGA) in the temperature range of 800° to 1,100° C. The ranking of the reductants, in order of decreasing reducing potential, is $H_2$, CO, and $CH_4$ at temperatures between 800° and 1,000° C; however, $CH_4$ became a better reductant than CO at 1,100° C. Water vapor did not decrease the reduction rate as much as did $CO_2$. Carbon deposition was observed at temperatures below 1,000° C with gas mixtures with high CO and low $H_2$ concentrations. With low-Btu gas at 900° C, over 90 pct of the iron oxide was reduced to iron in less than 3 h. This compares with a reduction time of 1.5 h with medium-Btu gas and 1 h with reformed natural gases.


[1]Research chemist.
[2]Supervisory physical scientist.
[3]Supervisory metallurgist.
Twin Cities Research Center, Bureau of Mines, Minneapolis, MN.



BEST COPY AVAILABLE

## INTRODUCTION

The Bureau of Mines, as part of its mission to investigate alternative technologies for processing domestic iron ores, conducted research to determine the reducibility of iron oxide pellets using different gaseous coal-based reductants. The most successful commercial direct-reduced iron (DRI) processes are natural gas based (10).[4] However, reductants made from natural gas and liquid fuels are becoming more costly, and their stable domestic supply for such applications is limited. To allow commercialization of DRI processes in the United States, information must be obtained so that coal-based DRI processes can be developed.

During the past several years, the Bureau of Mines (at its Twin Cities Research Center) has operated a single-stage, fixed-bed, air-blown gasifier with bituminous, subbituminous, and lignite coals (16) to generate a low-Btu gas for metallurgical application. The $H_2$ and CO contents of this gas are lower than those of the gas produced by oxygen-blown gasifiers (table 1). For purposes of comparison, the gas compositions from other gasifiers and other sources are also shown in table 1, along with gas codes and some definitions of the terms used in this report.

Considerable research has been conducted on the reduction kinetics of iron oxides with single-component gas reductants (6), but very few data are available regarding experimental reduction kinetics using complex gas mixtures such as would be produced by coal gasification. A report (11) was published recently on the reduction of iron oxide pellets with low-Btu gas, but it mainly dealt with the inhibiting influence of hydrogen sulfide on reduction.

Since only very limited data are available on the iron oxide reducibility potential of coal (producer) gases, a research program was initiated to develop an experimental model whereby the reduction rate could be predicted from the gas composition and temperature. Reduction kinetic data were obtained first with single-reductant gas mixtures and then with more complex multireductant gas mixtures. In some tests, the pellet compression strengths and porosities were also evaluated before and after reduction.

[4]Underlined numbers in parentheses refer to items in the list of references at the end of this report.

TABLE 1. - Partial analyses of actual and simulated reducing-gas mixtures

| Gas code | Type of gas mixture | Chemical analysis, pct | | | | | | | | Reference |
|---|---|---|---|---|---|---|---|---|---|---|
| | | $H_2$ | CO | $CH_4$ | $CO_2$ | $H_2O$ | $H_2+CO+CH_4$ | $CO_2+H_2O$ | $N_2$ | |
| ACTUAL FURNACE GASES | | | | | | | | | | |
| LAG.. | Lignite air gasifier..... | 20 | 27 | 2 | 7 | 21 | 49 | 28 | 23 | 16 |
| COG.. | Coal oxygen gasifier..... | 33 | 59 | 1 | 7 | 1 | 93 | 8 | 0 | 2 |
| CCO.. | Coal-$CO_2$ acceptor..... | 59 | 15 | 14 | 9 | 1 | 88 | 10 | 2 | 4 |
| RNGR. | Reformed natural gas (recycled) | 49 | 47 | 1 | 1 | 2 | 97 | 3 | 0 | 4 |
| RNG.. | Reformed natural gas..... | 71 | 23 | 1 | 1 | 4 | 95 | 5 | 0 | 4 |
| SIMULATED COMPLEX GAS MIXTURES | | | | | | | | | | |
| L-Btu | Low-Btu[1]..... | 20 | 27 | 2 | 7 | 0 | 49 | 7 | 44 | 16 |
| M-Btu | Medium-Btu[1]..... | 37 | 47 | 3 | 13 | 0 | 87 | 13 | 4 | 2 |
| RF-1. | Reformed gas-1..... | 50 | 48 | 1 | 1 | 0 | 99 | 1 | 0 | 4 |
| RF-2. | Reformed gas-2..... | 55 | 35 | 3 | 7 | 0 | 93 | 7 | 0 | 4 |
| RF-3. | Reformed gas-3..... | 73 | 13 | 5 | 9 | 0 | 91 | 9 | 0 | 4 |

[1]Low-Btu = 85 to 200 Btu/scf; medium-Btu = 260 to 325 Btu/scf (2).

BEST COPY AVAILABLE

ACKNOWLEDGMENTS

The authors wish to express their gratitude to Jeff A. Aldinger for his help with the reduction tests, and Edward J. Helmueller, who determined the physical properties of the pellets. Both of these were students employed at the Twin Cities Research Center during the summer of 198[illegible].

## EXPERIMENTAL WORK

### MATERIALS

The iron oxide pellets used in this research were commercially produced from a magnetite concentrate. The pellets were sized to minus 1/2 in (12.7 mm) and plus 7/16 in (11.1 mm). Several hundred sized pellets were further classified by weight in the range of 3.1 to 3.4 g. Typical analyses of the pellets are shown in table 2. The percent oxygen was 28.5 as determined by the weight loss at 100-pct reduction; in this report, it was assumed that the weight loss was proportional to the percent reduction. The pellet strength of 20 pellets before reduction was 293±138 lb (133±63 kg); the first value is the mean value, and the second value is the standard deviation. Some of the other pellet properties before reduction follow: porosity = 24±4 pct, and pore diameter at 50 pct pore volume = 4.0±0.9 μm. The porosity value only includes the surface-connected open pores and those accessible by the mercury porosimeter technique. The true density of the pellet, ground to 100 pct minus 325 mesh, was 4.9±0.2 g/cm$^3$.

TABLE 2. - Percentage chemical analyses of fired iron oxide pellets before reduction

| Chemical | Pct | Chemical | Pct |
|---|---|---|---|
| $Fe_T$[1] | 66.3 | $Na_2O$ | 0.03 |
| $Fe^{2+}$ | .3 | $K_2O$ | .02 |
| $SiO_2$ | 3.0 | $TiO_2$ | .8 |
| $Al_2O_3$ | .6 | C | .2 |
| CaO | .9 | P | .12 |
| MgO | .3 | S | .01 |
| $MnO_2$ | .06 | | |

[1]Total iron content.

### PROCEDURE

For each test, one iron oxide pellet was selected at random from a large batch of indurated pellets. Before and after each test, the pellet diameter and weight was determined. During the test, the pellet was held in a platinum wire-mesh basket (fig. 1) suspended with a platinum chain from the left pan of an automatic recording balance (sensitivity and reproducibility better than ±0.002 g).

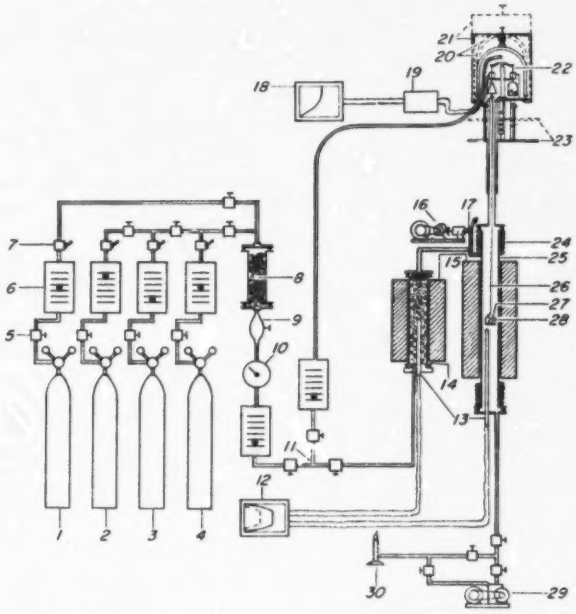


FIGURE 1. - Experimental equipment used in reduction studies of iron oxide pellets.

BEST COPY AVAILABLE

Chemically pure (>99.9 pct) single-component or premixed gases were metered into the gas preheater and then to the thermogravimetric analysis apparatus. The furnace pressure was 1 atm and the total flow rate was 1.5 SLM, unless otherwise stated. Ten percent of this gas was not preheated but was used to flush the bell jar before the gas entered the pellet reactor chamber (80-cm-long, 5-cm-diam alumina tube). Before the heat was turned on, the reactor chamber and balance unit were evacuated to 0.1 atm and then backfilled with nitrogen. This procedure was repeated three times. The reactor was heated in 1 SLM nitrogen gas to within 5° C of the desired operating temperature before the balance platform was lowered to place the pellet in the 10-cm-long hot zone. Five minutes after the pellet was lowered into the hot zone, the nitrogen flow was shut off and the reducing gas flow was started. Unless otherwise stated, the reducing-gas flow was maintained until no further weight loss was observed, or for a maximum of 4 h. After this time, the nitrogen flow was turned on and the pellet was raised into the cold zone. The power to the furnace then was turned off, and, after the furnace was flushed for 2 h, the nitrogen gas lines closed.

## RESULTS AND DISCUSSION

### SINGLE-REDUCTANT GAS MIXTURES

The reduction rates were first determined with the single-gas reductants (100 pct $H_2$, CO, or $CH_4$). The temperature of 900° C was selected for the baseline tests. With the 100 pct $H_2$ gas, the reduction rate increased with the increasing flow rates from 0.3 to 1.5 SLM, but between 1.5 and 4.4 SLM, very little change in the reduction rate was observed (fig. 2). With 100 pct CO or $CH_4$, a flow of 0.8 SLM was fast enough to reach the critical flow rate. In the tests conducted at temperatures higher than 900° C, the gas flows were 2.3 SLM with 100 pct $H_2$ and 1.5 SLM with all the other gases.

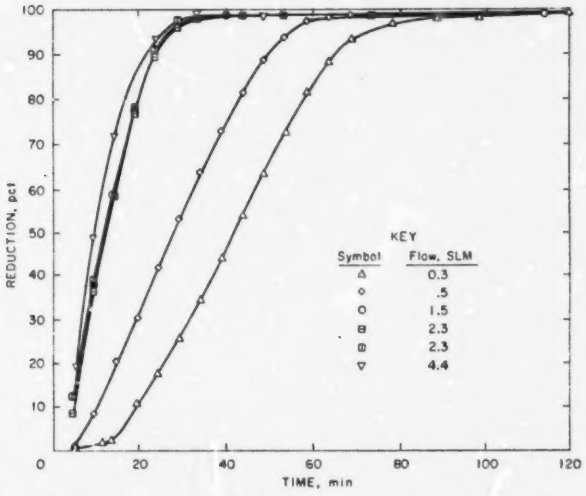


FIGURE 2. - Influence of gas flow rates on percent reduction with 100 pct $H_2$ at 900° C.

The reduction data with 100 pct $H_2$ gas at 900° C were used to determine the best equation for subsequent comparison of different reductants. Hydrogen was chosen as the baseline reductant because it was expected to be the best reductant, and one would expect the least number of complicating side reactions. The normalized weight-loss (percent-reduction) data were expressed in various forms using different equations; the values from the left side of the equation (y) versus time are shown in figure 3. Straight-line regression correlations were calculated for reduction values ranging from 10 to 90 pct and are shown as dashed lines. The weight-loss data obtained on the strip-chart recorder can be expressed by equation 1:

$$R/100 = A(t) + B, \qquad (1)$$

where R is the percent reduction, A is the slope, t is the time in minutes, and B is a constant. A low correlation coefficient of 0.940 was obtained with this equation. A much higher correlation coefficient of 0.993 was obtained using equation 2:

$$[1 - (1-R/100)^{1/3}] = k_e (t) + C, \qquad (2)$$

BEST COPY AVAILABLE

where $k_e$ is the experimental rate constant in reciprocal minutes, and C is a constant. The theoretical basis of equation 2 is the assumption that the chemical reaction at the receding interfacial shell surface is the rate-controlling mechanism (15, 18). If the rate-controlling mechanism was solely the gaseous diffusion through the product layer, then the time dependence of the degree of reduction of a sphere should follow the parabolic law (17), which can be expressed by equation 3:

$$1/2 - R/300 - 1/2\,(1-R/100)^{2/3} = k'\,(t) + D, \qquad (3)$$

where k' is the parabolic rate constant, and D is a constant. Equation 3 produced a lower correlation coefficient (0.986) than did equation 2. Turkogan (19) reported that the rate-controlling step depends essentially on the uniform internal reaction on the pore walls, and they obtained a good fit with equation 4:

$$\log\,(1 - R/100) = -\,k''\,(t) + E, \qquad (4)$$

where k" is the first-order rate constant in reciprocal minutes, and E is a constant. With equation 4, the correlation coefficient was 0.987.

The highest correlation coefficient was obtained with equation 2, and therefore this equation was used to compare the results in this report. Figure 3 also shows that this equation fits the data better than the other equations even up to about 95-pct reduction.

With 100 pct $H_2$, CO, or $CH_4$ gas, the dependence of the rate constants ($k_e$) on temperature was determined at 800°, 900°, 1,000°, and 1,100° C; the results are shown in the Arrhenius plot (fig. 4). The apparent activation energies were calculated using the following equation:

$$\log k_e = \frac{\Delta H^*}{4.575}\,(10^3/T) + F, \qquad (5)$$

where $\Delta H^*$ is the apparent activation energy in kilocalories per mol, T is the temperature in kelvins, and F is a constant. The influence of temperature on the activation energies was calculated by the least-squares regression method, and the values for 100 pct $H_2$, CO, and $CH_4$ were 14.2, 13.7, and 40.6 kcal/mol,

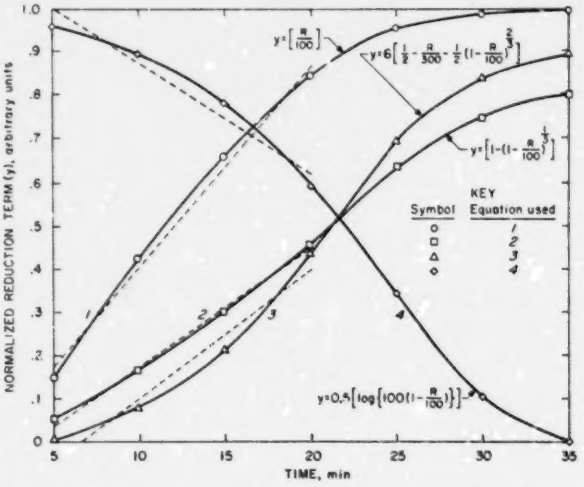


FIGURE 3. - Comparison of reduction-rate data using various normalized reduction functions (the best fit straight lines between 10- and 90-pct reduction are shown as dashed lines).

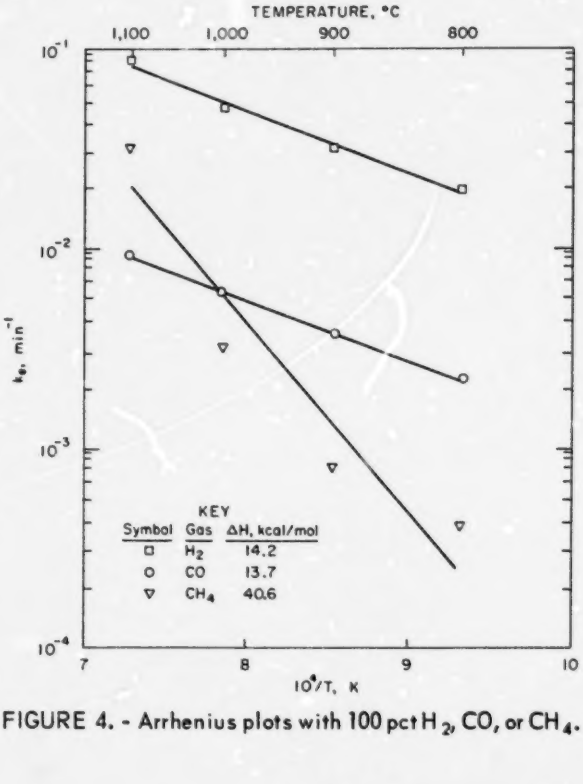


FIGURE 4. - Arrhenius plots with 100 pct $H_2$, CO, or $CH_4$.

BEST COPY AVAILABLE

respectively. These values are in fair agreement with those of other investigators. Kurgina (13) reported values of 14.5 and 17.3 kcal/mol for $H_2$ and CO, respectively. Hansen (6) obtained values of 10.8 kcal/mol with $H_2$ and 11.5 kcal/mol with CO using a red iron ore from Alabama. However, earlier work by his group (8) reported a value of 15.3 kcal/mol with $H_2$ using a different iron ore from Minnesota. The activation energy with $CH_4$ was considerably higher, but Mazhenov (14) also reported a high value (43.0 kcal/mol).

The results in figure 4 show that 100 pct $H_2$ is a much better reductant than is 100 pct CO, which is in agreement with other investigators (8, 12). One-hundred-percent $CH_4$ is a poor reductant at 800° C, but at 1,100° C, it is between CO and $H_2$.

Reduction rates were then determined with reductants diluted with $N_2$ at 900° C, and the total flow was kept constant at 2.3 SLM. Figure 5 shows the curves for the logarithm of the reductant partial pressure versus logarithm of the reduction rate. Fairly linear curves were obtained and the lines were defined by equation 6:

$$\log k_e = z \log P_r + G, \qquad (6)$$

where z is the exponent of the reductant partial pressure, $P_r$ is the partial pressure of the reductant in atmospheres, and G is a constant. The values for z with $H_2$, CO, and $CH_4$ were 1.60, 0.59, and 1.80, respectively.

Different partial pressures of CO and $H_2$ were also obtained by dilution with $CO_2$ and water vapor, respectively. Water vapor and $CO_2$ are not only diluents but also oxidants, which can cause the reduction reactions to reverse. Al-Kahtany (1) reported that when oxidants are present with reductants, a mathematical function of the partial pressure of the oxidant must be subtracted from the partial pressure of the reductant for determining the reaction rate constants.

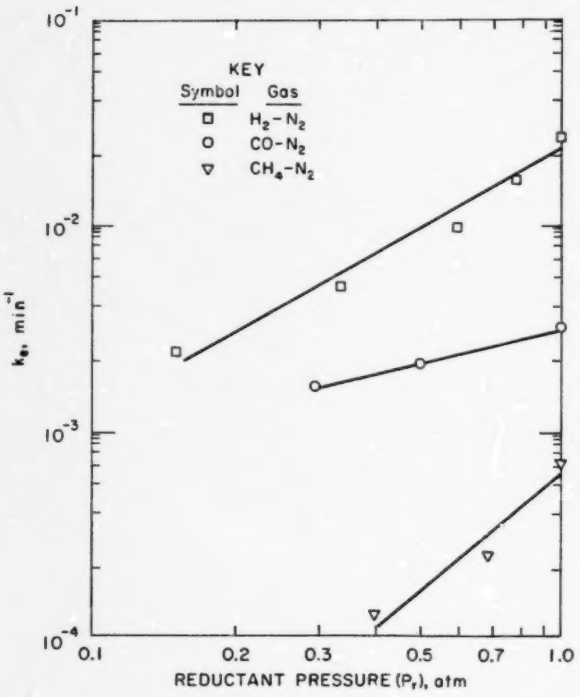


FIGURE 5. - Plot of logarithm of reductant pressure and reduction rate at 900° C.

The results obtained by adding $CO_2$ to CO are shown in figure 6. It can be seen from these results that the two duplicate CO tests are similar, but increasing the oxidant pressure ($P_o$) retards the reduction rates. With 40 pct $CO_2$ in CO, the curve levels off at about 30-pct reduction. The conversion from hematite to wustite ($Fe_xO$, where x ranges between 0.83 and 0.95) corresponds to about a 30-pct reduction; with this gas mixture at 900° C, the reduction to metallic iron does not seem to occur. These results are in agreement with thermodynamic data shown in figure 7. The reduction rate constants for the $CO_2$ additions to CO gas mixtures are plotted in figure 8. The calculated $CO-CO_2$ rate curve indicates that a fairly good fit was obtained with equation 7:

$$k_{CO-CO_2} = 0.18 \left[ 7.0 \, (P_{CO})^{0.59} - \frac{P_{CO_2}}{0.01 + 0.19 \, P_{CO_2}} \right] e^{-13,700/RT}, \qquad (7)$$

BEST COPY AVAILABLE

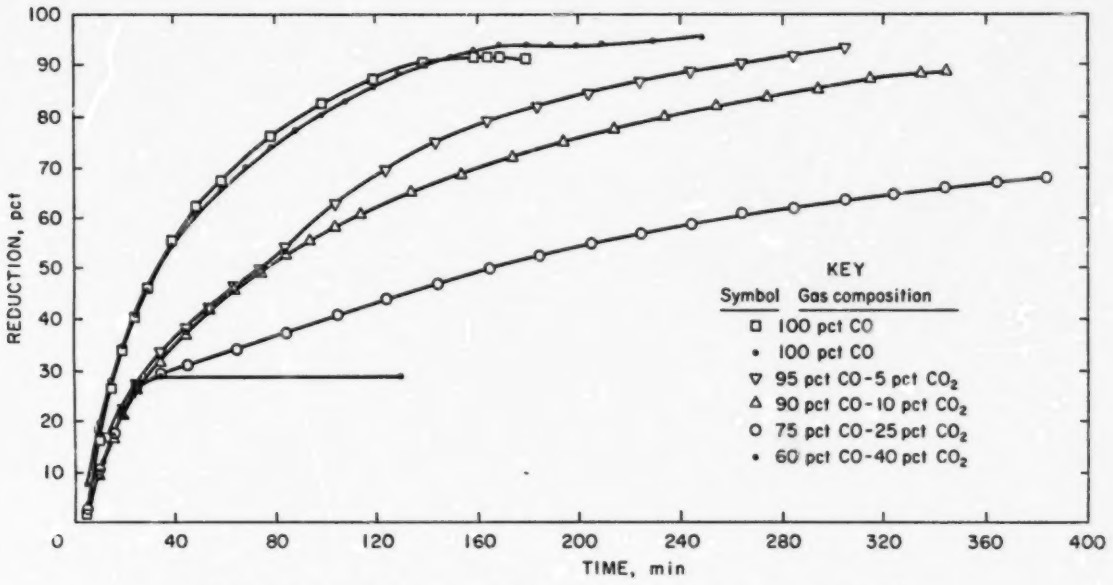


FIGURE 6. - Influence of $CO_2$ and CO on reduction at 900° C.

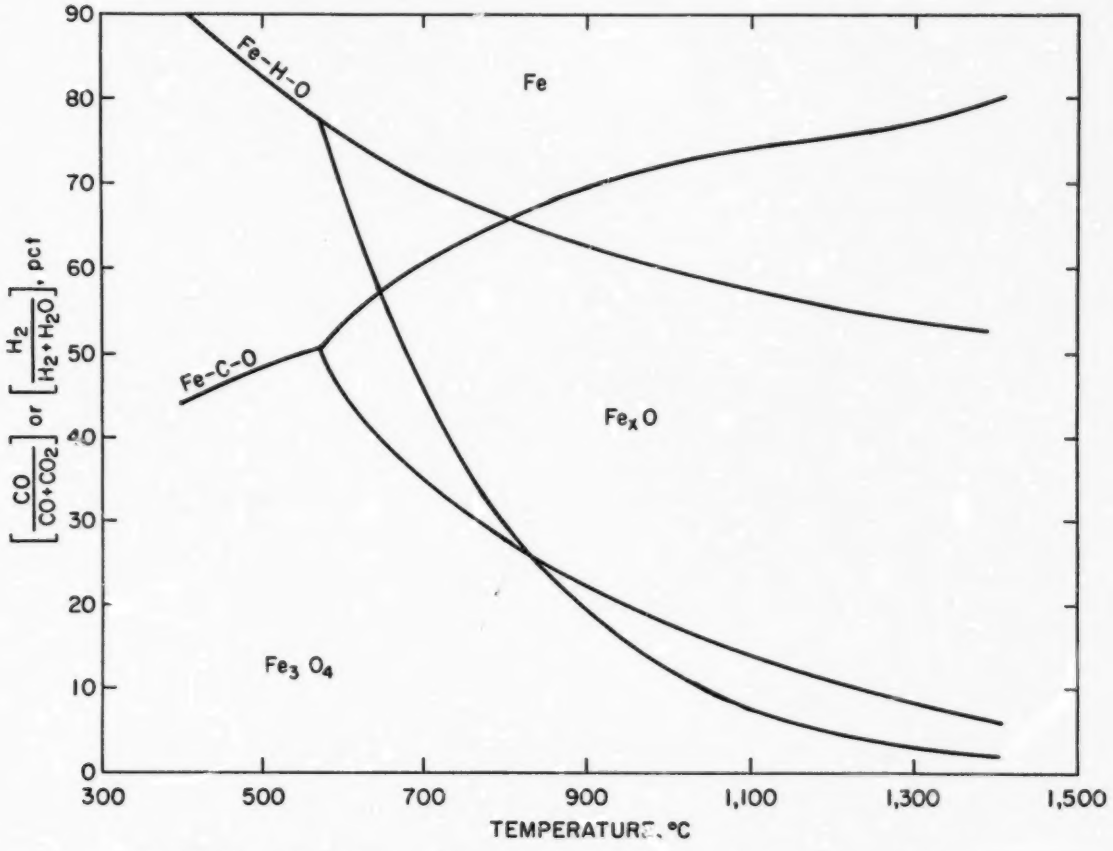


FIGURE 7. - Equilibrium diagram of iron in presence of various gases (7).

BEST COPY AVAILABLE

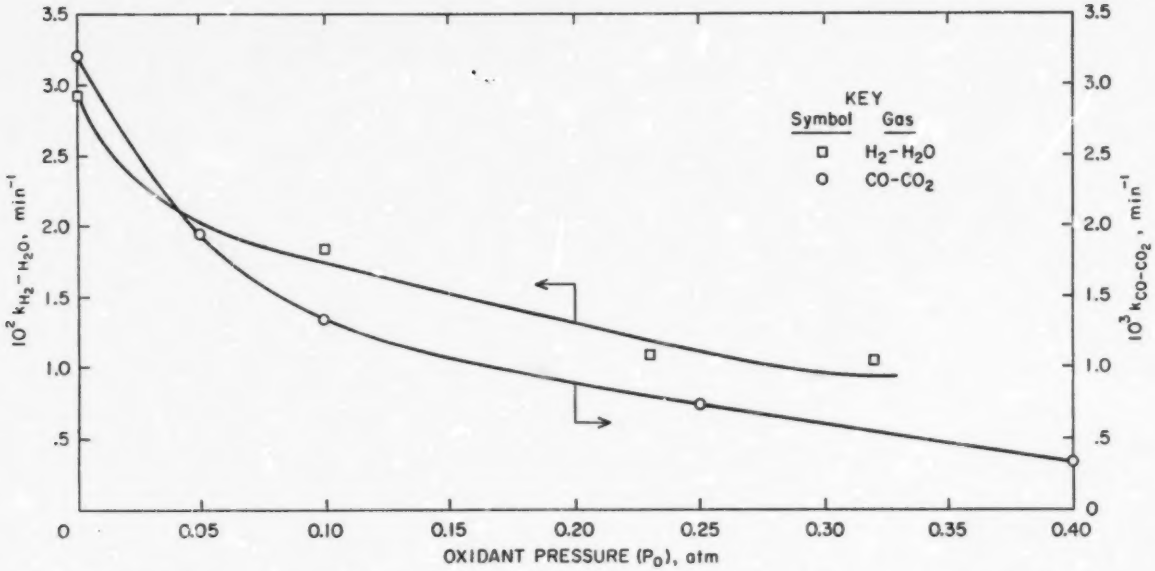


FIGURE 8. - Influence of water vapor and $CO_2$ on reduction rate constant at 900° C.

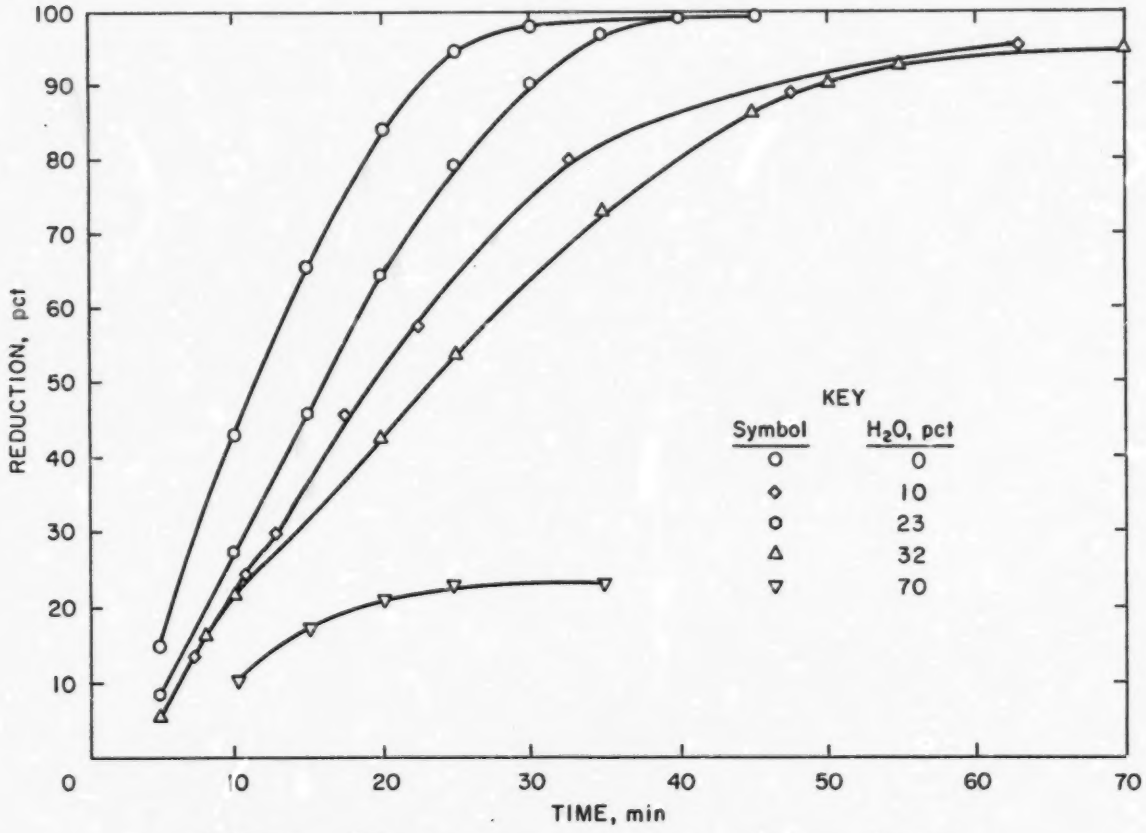


FIGURE 9. - Influence of water vapor in $H_2$ on reduction at 900° C.

BEST COPY AVAILABLE

where $k_{CO-CO_2}$ is the rate constant for $CO-CO_2$ reduction reaction, and $P_{CO_2}$ is the partial pressure of $CO_2$ in atmospheres. This semiempirical equation was obtained by trying different constants until a fairly good fit was obtained. The deviations of the experimental rates from the values calculated from this equation were 5 pct or less in the range of 0 to 25 pct $CO_2$. In developing this equation, the assumptions were made that the activation energy and the exponent for the partial pressure of the reductant did not change as the oxidant content was increased. The assumption was also made that the constants were independent of temperature in the range from 800° to 1,100° C. No conclusive mechanism is implied by the magnitude of these constants and the form of this equation.

The effect of water vapor in $H_2$ on the iron oxide reduction rate at 900° C was also determined (fig. 9). It is evident from these results that water retards the reduction rate. With 70 pct water vapor, the reduction leveled off below 30 pct. This suggests that the reduction stopped at wustite and did not proceed to metallic iron, which was expected from the data shown in figure 7. The reduction rate constants were calculated with water vapor added to $H_2$, and the data were plotted in figure 8. The calculated $H_2-H_2O$ curve indicates that a fairly good fit was obtained with equation 8:

$$k_{H_2-H_2O} = 0.22\left[60(P_{H_2})^{1.6} - \frac{P_{H_2O}}{0.0005 + 0.06\ P_{H_2O}}\right] e^{-14,200/RT}, \qquad (8)$$

where $k_{H_2-H_2O}$ is the rate constant for the $H_2-H_2O$ reduction reaction, and $P_{H_2O}$ is the partial pressure of water in atmospheres. The deviations of the experimental rates from the values calculated from this semiempirical equation were 6 pct or less in the range of 0 to 23 pct $H_2O$.

## SIMULATED REFORMED AND COAL GAS MIXTURES

The tests discussed earlier in this report were conducted with gases containing only one or two components, but commercial processes use more complex gas mixtures containing predominantly $H_2$, CO, $CH_4$, $CO_2$, and water vapor. (See table 1.) Several cylinders of simulated complex gas mixtures were purchased for determining the reduction rates at various temperatures. Table 3 shows the experimental and calculated rate constants for both the single-reductant and complex gas mixtures. By combining the previously developed equations and data, the calculated rate constants ($k_c$) for the complex gases were obtained by using equation 9:

$$k_c = 0.22\left[60(P_{H_2})^{1.6} - \frac{P_{H_2O}}{0.0005 + 0.06\ P_{H_2O}}\right] e^{-14,200/RT}$$

$$+ 0.18\left[7.0\ (P_{CO})^{0.59} - \frac{P_{CO_2}}{0.01 + 0.19\ P_{CO_2}}\right] e^{-13,700/RT}$$

$$+ 2.3 \times 10^4\left[(P_{CH_4})^{1.8}\right] e^{-40,600/RT}. \qquad (9)$$

BEST COPY AVAILABLE

TABLE 3. - Chemical and physical properties of reduced iron oxide pellets[1]

| Gas temp., °C | Partial chemical analysis, pct | | Carbon, pct | Swelling[2] (100 $V_f$/$V_i$), pct | Strength,[3] kg | $r_{40}$,[4] pct/min | Reaction rate, min | | Time, min[5] | |
|---|---|---|---|---|---|---|---|---|---|---|
| | $Fe_T$, Fe° | 100 Fe°/$Fe_T$ | | | | | $10^2$ $k_e$ | $10^2$ $k_c$ | $t_{90}$ | $t_{max}$ |
| $H_2$: | | | | | | | | | | |
| 800 | 92.7 87.1 | 94 | 0.1 | 10 | 97 | 4.2 | 1.83 | 1.72 | 30 | 85 |
| 900 | 92.5 89.1 | 96 | .1 | ND | 59 | 5.2 | 2.95 | 3.03 | 25 | 35 |
| 1,000 | 92.7 91.3 | 98 | ND | 13 | 41 | 8.4 | 4.61 | 4.89 | 15 | 20 |
| 1,100 | 90.0 88.3 | 98 | .1 | 22 | 41 | 16.8 | 8.01 | 7.36 | 8 | 10 |
| CO: | | | | | | | | | | |
| 800 | 68.1 56.3 | 83 | 5.3 | ND | ND | .5 | .22 | .21 | ND | 160 |
| 900 | 90.1 84.8 | 94 | 2.2 | 10 | 100 | 1.1 | .35 | .35 | 140 | 140 |
| 1,000 | 90.8 88.4 | 97 | 2.4 | 10 | 97 | 1.5 | .55 | .56 | 90 | 135 |
| 1,100 | 90.8 87.5 | 96 | 1.0 | 32 | 43 | 2.3 | .90 | .83 | 45 | 80 |
| L-Btu: | | | | | | | | | | |
| 800 | 92.4 87.2 | 94 | .2 | ND | ND | .1 | .25 | .14 | 215 | 240 |
| 900 | 91.1 85.4 | 94 | .1 | 21 | ND | .4 | .33 | .24 | 155 | 240 |
| 1,000 | 91.1 85.9 | 94 | .1 | ND | ND | .9 | .39 | .39 | 132 | 240 |
| 1,100 | 90.8 87.6 | 96 | .2 | 30 | 23 | 2.1 | .83 | .59 | 55 | 75 |
| M-Btu: | | | | | | | | | | |
| 800 | 90.4 83.0 | 92 | .5 | ND | ND | 1.1 | .48 | .37 | 115 | 200 |
| 900 | 91.5 85.0 | 93 | .4 | ND | ND | 1.2 | .51 | .66 | 95 | 140 |
| 1,000 | 91.3 86.3 | 95 | .3 | ND | ND | 1.5 | .77 | 1.06 | 70 | 85 |
| 1,100 | 93.0 88.3 | 95 | .1 | ND | ND | 2.8 | 1.63 | 1.59 | 35 | 45 |
| RF-1: | | | | | | | | | | |
| 800 | 89.4 77.1 | 86 | 1.6 | ND | ND | 1.6 | .67 | .67 | 90 | 85 |
| 900 | 93.0 86.4 | 93 | 1.2 | ND | ND | 2.9 | 1.22 | 1.17 | 50 | 75 |
| 1,000 | 93.7 89.8 | 96 | .8 | ND | ND | ND | 1.68 | 1.89 | 30 | 40 |
| 1,100 | 92.3 92.1 | 100 | .2 | 22 | ND | 5.1 | 2.55 | 2.83 | 20 | 30 |
| RF-2: | | | | | | | | | | |
| 800 | 91.5 88.4 | 97 | .3 | 10 | 104 | 2.0 | .88 | .69 | 65 | 90 |
| 900 | 90.6 85.9 | 95 | .4 | 10 | 63 | 3.1 | 1.31 | 1.21 | 55 | 80 |
| 1,000 | 92.3 89.6 | 97 | .3 | 10 | 59 | 4.5 | 2.20 | 1.95 | 25 | 60 |
| 1,100 | 91.7 88.8 | 97 | .2 | 16 | 18 | 7.5 | 3.36 | 2.94 | 15 | 20 |
| RF-3: | | | | | | | | | | |
| 800 | 91.7 89.6 | 98 | .1 | 10 | ND | 2.2 | .87 | 1.03 | 60 | 125 |
| 900 | 89.0 85.7 | 96 | .1 | 10 | ND | 4.2 | 1.66 | 1.81 | 35 | 85 |
| 1,000 | 89.2 85.9 | 96 | .2 | 10 | 50 | 4.4 | 2.33 | 2.93 | 25 | 65 |
| 1,100 | 91.2 88.8 | 97 | .2 | 26 | 23 | 6.7 | 4.59 | 4.42 | 10 | 15 |
| $CH_4$: | | | | | | | | | | |
| 800 | 73.4 38.2 | 52 | 10.3 | 106 | 50 | ND | .04 | .02 | ND | 240 |
| 900 | 67.6 64.9 | 96 | 26.8 | 106 | 4 | ND | .08 | .07 | ND | 240 |
| 1,000 | 66.0 64.3 | 97 | 26.9 | 101 | 4 | ND | .30 | .25 | ND | [6]80 |
| 1,100 | 63.9 63.0 | 99 | 29.0 | ND | ND | 5.2 | 2.99 | .81 | 20 | [6]25 |

ND Not determined.

[1]Reduction time was 4 h or until a maximum weight loss was observed.

[2]Swelling was defined as the ratio of 100 $V_f/V_i$ where $V_i$ and $V_f$ refer to the initial and final pellet, volume, respectively.

[3]Unconfined compressive strength of reduced pellets.

[4]The term $r_{40}$ was defined as the slope of curve (percent reduction with time) at 40-pct reduction according to equation 10.

[5]The terms $t_{90}$ and $t_{max}$ refer to the time for 90-pct reduction and maximum weight loss, respectively.

[6]The total times for the 1,000° to 1,100° C reduction were 120 and 360 min, respectively.

BEST COPY AVAILABLE

Good agreement was obtained between the calculated and the experimental rates for all gas mixtures, except for 100 pct $CH_4$ at 1,100° C, where the calculated $k_c$ was considerably lower than the experimental $k_e$ (table 3 and figure 10). This deviation is probably due to complex $CH_4$ reactions occurring at this temperature. For example, the products ($CO_2$ and water vapor) from reduction can react with $CH_4$ to produce $H_2$ and CO, or $CH_4$ can be decomposed to $H_2$ and carbon.

The temperature dependence of the reaction rate in the range of 800° to 1,100° C was also determined with the complex gas mixtures. The activation energies for L-Btu, M-Btu, RF-1, RF-2, and RF-3 were 15.5, 10.5, 12.6, 13.8, and 15.2 kcal/mol, respectively. The activation energies were similar to the values found for 100 pct $H_2$ and CO (fig. 4). This was expected since the methane concentrations were low in the complex gas mixtures.

Other methods for determining the relative reduction kinetics were also used rather than the specific rate constant in equation 10. One of these methods was based on the time required to reach 90-pct reduction, and these data are shown in the bar graph in figure 11. These relative reduction data are in agreement with the earlier results, which showed that the $H_2$ content in the complex gases (table 1) and the temperature were the two most important variables affecting the reduction kinetics. These data also show that the time required for 90-pct reduction for simulated low-Btu gas is about the same as for 100 pct CO, but that the effectiveness of medium-Btu coal gas is between that of 100 pct CO and the reformed natural gases (RF-1 to RF-3).

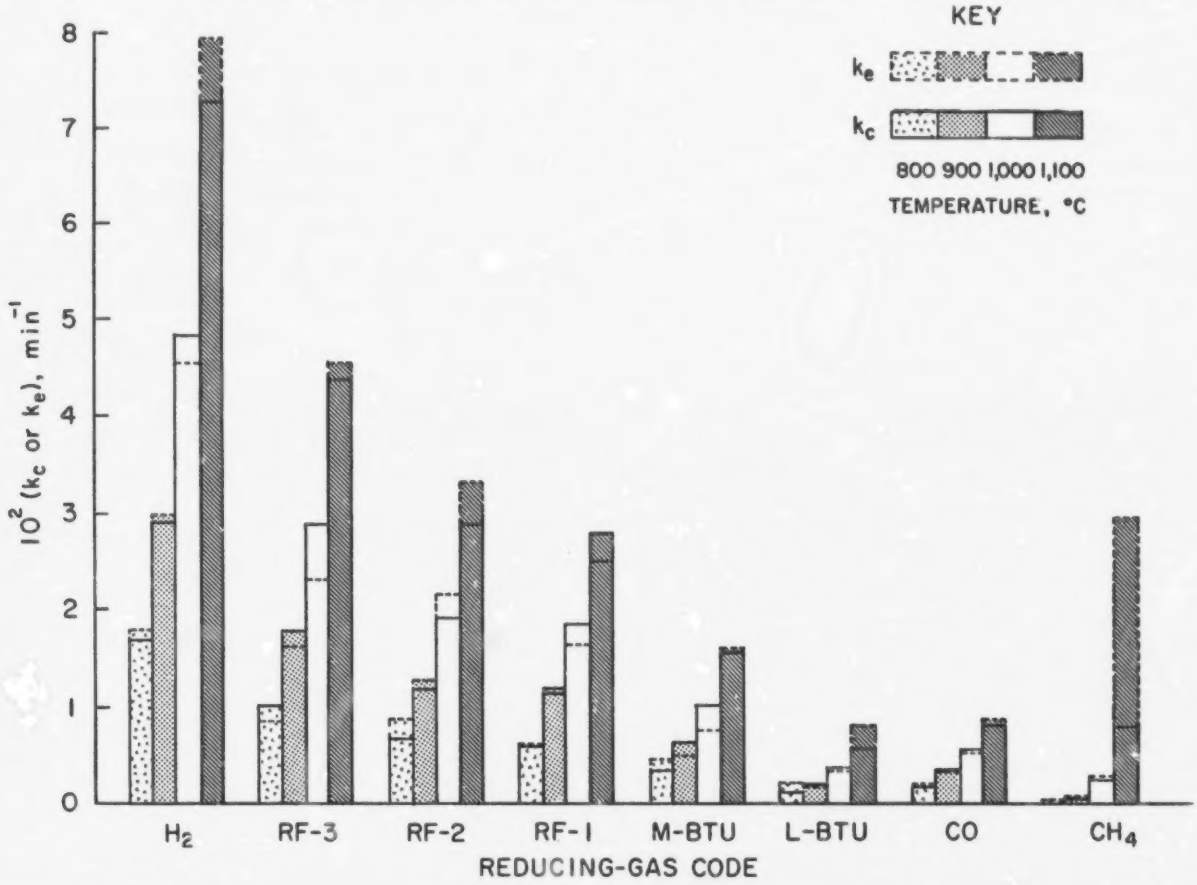


FIGURE 10. - Dependence of calculated and experimental reduction rate constants on gas composition and temperature.

BEST COPY AVAILABLE

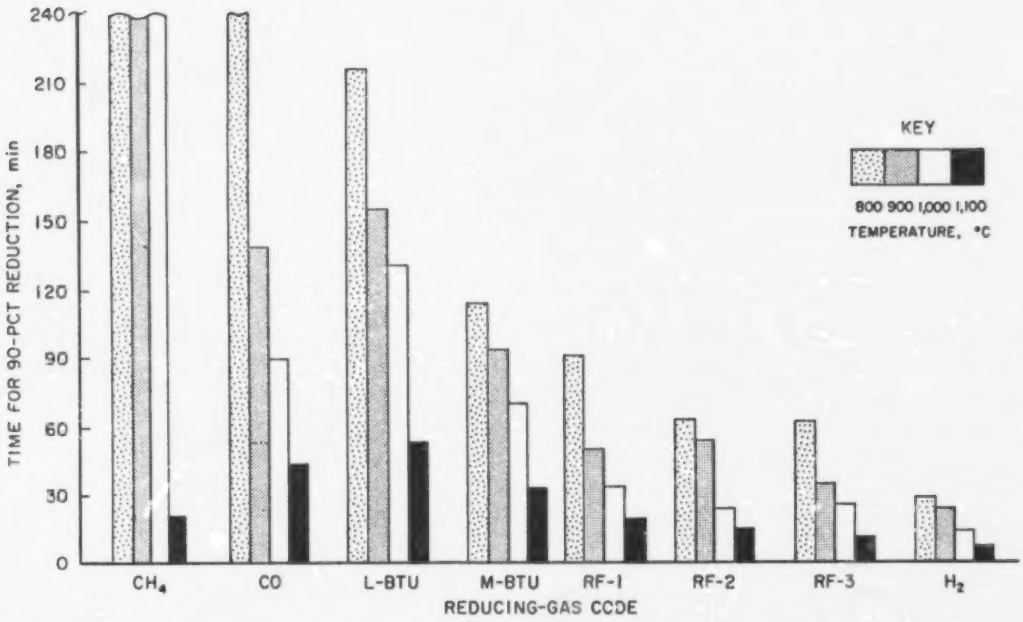


FIGURE 11. - Dependence of the 90-pct reduction time on type of reducing gas and temperature.

Another method (9) was also used to compare the relative reduction kinetics, which involves the slope of reduction-time curve at the 40-pct reduction ($r_{40}$) as determined by equation 10:

$$r_{40} = \frac{33.6}{(t_{60} - t_{30})}, \qquad (10)$$

where $t_{60}$ and $t_{30}$ refer to time in minutes to obtain 60- and 30-pct reduction, respectively. The $r_{40}$ values in table 3 were in agreement with the results discussed earlier, which showed the strong dependence of the reduction rate on temperature and $H_2$ content of the gas. Similar relative reduction observations were made by comparing the time required for maximum weight loss and 90-pct metallization (table 3). However, these two methods were not as good as the $r_{40}$ method because 90-pct metallization and maximum weight loss were not reached in some cases. For example, a test using 100 pct $CH_4$ at 800° C did not meet these criteria even after 350 min.

## EVALUATION OF REDUCED PELLETS

Chemical and physical properties of the pellets reduced with the different gas mixtures are shown in table 3. More residual oxygen was retained in the pellet at the lower temperatures for the same reduction time, as shown by the percent metallization (100 $Fe°/Fe_T$). The percent carbon was the greatest with the $CH_4$- and CO-rich gases at the lowest temperatures. With 100 pct CO (or $CH_4$), the reduced pellets were black, rather than the normal gray, and had low compressive strengths. Earlier research in the Bureau's Twin Cities laboratory showed that the black coating was carbide and elemental carbon (5). Mazhenov (14) also reported the deposition of carbon when 100 pct $CH_4$ was used. The pellets that contained high carbon (over 10 pct) also had high swelling values.

The porosity of the pellets was determined before and after reduction. The results shown in figure 12 indicated that the pore volume with the reduced pellets was considerably greater than with the indurated iron oxide pellets before reduction. The total porosity of the reduced pellets was over 40 pct, while that of the oxide pellets was 21 pct. The pellets reduced with 100 pct $H_2$ appeared to have more micropores (i.e., 1.5 μm) than those reduced with 100 pct CO or low-Btu gas. This possibly can be

BEST COPY AVAILABLE

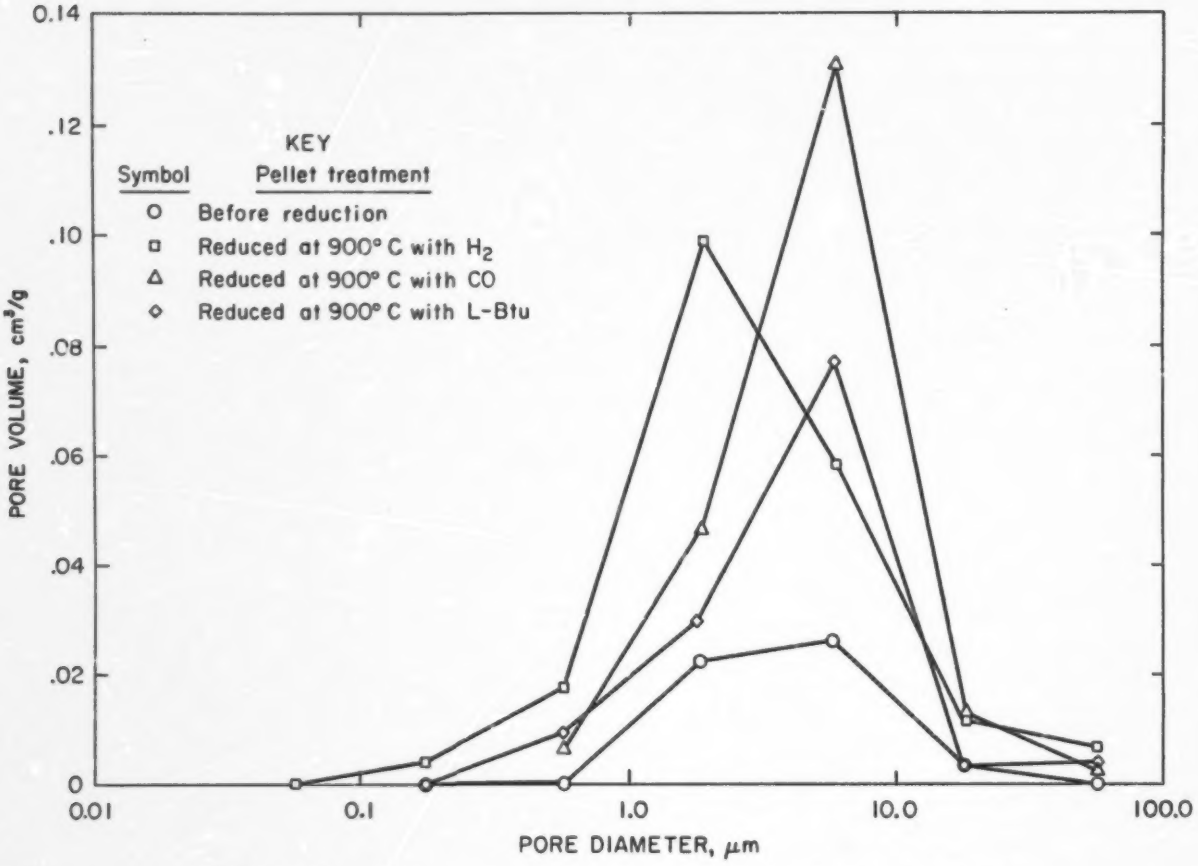


FIGURE 12. - Pellet pore size distribution before and after reduction.

explained by carbon deposition being favored with rich carbon monoxide gases and the elemental carbon plugging up the pores. Microscopic examination of the iron layer surrounding the residual iron oxide core indicated that the iron was very porous. Therefore, one would suspect that mass transfer through the product layer was not the rate-controlling mechanism. This supports the earlier finding that a better fit was obtained with the topochemical rate equation (eq. 2) than with the gas diffusion equation (eq. 3).

## CONCLUSIONS

This comparative study showed that the relative reduction rates are extremely dependent on the composition and temperature of the simulated coal gas. A semi-empirical model was developed to correlate the gas composition and temperature with the specific reduction rates at a total gas pressure of 1 atm. The exponent for the $H_2$ partial pressure term in the rate equation was about twice those of CO. Water vapor did not decrease the reduction rate as much as did $CO_2$. At low temperatures, all reductants contributed significantly to the reduction rate except $CH_4$, which did so only at a high temperature (1,100° C). The time required to obtain 90-pct reduction with the low-Btu gas mixture was slightly longer than with 100 pct CO. With medium-Btu gas, less time was required than with 100 pct CO, but more time was required than with reformed natural gas or 100 pct $H_2$. The temperatures required to reach 90-pct reduction in about 1 h

BEST COPY AVAILABLE

with different gas mixtures were 800° C for 100 pct $H_2$, 800° C for RF-3, 900° C for RF-1 and -2, 1,000° C for M-Btu, and 1,100° C for L-Btu, 100 pct CO, and 100 pct $CH_4$. Carbon deposition was most noticeable with the rich CO gases at 800° C and with rich $CH_4$ gases at all temperatures. At 900° C, over 90 pct of the iron oxide was reduced to iron in less than 3 h with low-Btu gas. This compares to a reduction time of 1.5 h with medium-Btu gas and 1 h with reformed natural gases.

## REFERENCES


1. Al-Kahtany, M. M., and Y. K. Rao. Reduction of Magnetite With Hydrogen: Part 1 - Intrinsic Kinetics. Ironmaking and Steelmaking, v. 7, No. 2, 1980, pp. 49-58.

2. Ashworth, R. A., K. C. Yvas, and D. G. Bonamer. Study of Low and Intermediate Btu Gas From Coal for Iron Ore Pelletizing (contract J0255021, Arthur G. McKee & Co.). BuMines OFR 36-77, 1977, 214 pp.; NTIS PB 264702.

3. Bjorkvall, B., and G. Thaning. Test Methods for Agglomerated Products - Part 1. Scand. J. Metall., v. 1, 1972, pp. 57-58.

4. Guseman, J. R. Fuels and Reductants. Ch. in Direct Reduced Iron Technology and Economics of Production and Use, ed. by R. L. Stephenson. Iron and Steel Soc., AIME, 1980, pp. 49-63.

5. Haas, L. A., S. E. Khalafalla, and P. L. Weston, Jr. Kinetics of Formation of Carbon Dioxide and Carbon From Carbon Monoxide in the Presence of Iron Pellets. BuMines RI 7064, 1968, 29 pp.

6. Hansen, J. P., J. E. Berryhill, and J. A. Aufman. Batch Reduction of Iron Ore in Fluidized Bed. BuMines RI 7461, 1970, 25 pp.

7. Hansen, J. P., T. N. Rushton, and S. E. Khalafalla. Reduction of Ferrous Oxide (Wustite) at High Temperature. BuMines RI 6712, 1966, 25 pp.

8. Hansen, J. P., T. N. Rushton, and C. W. Schultz. Reaction Interface Speed as a Reducibility Index for Iron Ore. BuMines RI 6827, 1966, 33 pp.

9. International Organization for Standardization. Iron Ores--Determination of Reducibility. ISO/DIS 4695, 1982, 8 pp.

10. Jackson, K. A. Metallized Pellets by the Hyl Process. Proc. Annu. AIME Meeting, MN Sec., Duluth, MN, Jan. 15-17, 1973, pp. 88-93.

11. Joyce, E. L., Jr., and K. Li. Reduction of Iron Ore Pellets in Simulated Low-Btu Gases. Trans. Iron and Steel Soc. AIME, Nov. 1984, pp. 61-64.

12. Kawai, M., H. Kimura, and T. Teramine. Reduction of Fine Iron Oxide by Carbon Monoxide, Hydrogen, and $C_3H_8$ Cracking Gas. Tetsu to Hagane, v. 46, No. 10, 1960, pp. 1130-32; Chem. Abstr., v. 61: 1166 2C.

13. Kurzina, T. P., and S. E. Filippov. Kinetics of the Reduction of Iron Oxides by Mixtures of Carbon Monoxide and Hydrogen. Izv. Vyssh. Uchebn. Zaved. Chern. Metall., v. 6, No. 9, 1963, pp. 5-10; Chem. Abstr., v. 60; 2573 b.

14. Mazhenov, M. A., D. I. Ryzhonkov, V. F. Knybsev, and S. I. Filippov. Kinetic Reduction Characteristics of Pelletized Iron Ore Carried Out by Means of Hydrogen and Methane. Izv. Vyssh. Uchebn. Zaved. Chern. Metall., v. 8, No. 7, 1965, pp. 11-15; Chem. Abstr., v. 63; 9526 c.

15. McKewan, W. M. Kinetics of Iron Oxide Reduction. Trans. Metall. Soc. AIME, v. 218, No. 2, 1960, pp. 2-6.

16. Nigro, J. C. Firing an Iron Ore Pelletizing Kiln With Low-Btu Gas From Lignite. BuMines RI 8670, 1982, 22 pp.

17. Nigro, J. C., T. D. Tiermann, and C. Prasky. Kinetics of CO Reduction of Hematite to Magnetite and Effect of Silica. BuMines RI 7720, 1973, 43 pp.

18. Nigro, J. C., R. K. Zahl, and C. Prasky. Effect of Dolomitic Lime on Magnetite Taconite Pellets. Trans. Soc. Metall. Eng. AIME, v. 254, 1973, pp. 328-336.

19. Turkdogan, E. T., and J. V. Vinters. Gaseous Reduction of Iron Oxides, Part III Reduction - Oxidation of Porous and Dense Iron Oxides and Iron. Metall. Trans., v. 3, 1972, pp. 1561-1574.


☆U.S. GPO: 1985-605-017/20,129

INT.-BU.OF MINES,PGH.,PA. 28149

BEST COPY AVAILABLE